INSTITUTE OF PHYSICS PUBLISHING JOURNAL OF PHYSICS: CONDENSED MATTER

J. Phys.: Condens. Matter **15** (2003) 3531–3537 PII: S0953-8984(03)57997-8

Phase evolution and its effect on magnetic properties of $Nd_{60}Al_{10}Fe_{20}Co_{10}$ bulk metallic glass

Lei Xia[1,2], Bing Chen Wei[3], Ming Xiang Pan[2], De Qian Zhao[2], Wei Hua Wang[2,4] and Yuan Da Dong[1]

[1] Institute of Materials, Shanghai University, Shanghai 200072, People's Republic of China
[2] Institute of Physics, Chinese Academy of Science, Beijing 100080, People's Republic of China
[3] National Microgravity Laboratory, Institute of Mechanics, Chinese Academy of Science, Beijing 100080, People's Republic of China

E-mail: whw@aphy.iphy.ac.cn

Received 8 January 2003, in final form 26 March 2003
Published 19 May 2003
Online at stacks.iop.org/JPhysCM/15/3531

Abstract

The thermal stability of nanocrystalline clusters, the phase evolution, and their effects on magnetic properties were studied for as-cast $Nd_{60}Al_{10}Fe_{20}Co_{10}$ alloy using differential scanning calorimetry curves, x-ray diffraction patterns, scanning electron microscopy, and high-resolution transition electron microscopy. Thermomagnetic curves and hysteresis loops of the bulk metallic glass were measured during the annealing process. The high thermostability of the hard magnetic properties of the samples observed is attributed to the stability of the nanocrystalline clusters upon annealing, while the slight enhancement in the magnetization is due to the precipitation of some Nd-rich metastable phases. The mechanism of thermostability of the nanocrystalline clusters and the formation of the metastable phases are discussed.

Annealing of metallic glasses causes changes in structure and physical properties due to atomic rearrangement and subsequent lowering of the free energy [1–4]. It is helpful for us to understand the dependence of the properties on the microstructural evolution of the amorphous alloys during heating. The recently developed bulk metallic glasses (BMGs) exhibit excellent glass-forming ability (GFA) and unique properties, and have been investigated intensively because of their significance in science and engineering [5–8]. More recently, Hays *et al* [9] reported that the *in situ* formed ductile dendritic crystalline phase improved the plastic strain to failure and other mechanical properties dramatically. This is somewhat similar to the case for $Nd_{60}Fe_{30}Al_{10}$ bulk glass-forming alloy [10]. As an important magnetic amorphous alloy system, Nd(Pr)–Fe(Co)–Al BMGs have evoked intensive interest due to their high coercivity, indicating their potential for use as permanent magnets. Among these, the $Nd_{60}Al_{10}Fe_{20}Co_{10}$

[4] Author to whom any correspondence should be addressed.

 © 2003 IOP Publishing Ltd Printed in the UK

BMG has shown high thermostability, good GFA, and, especially, higher coercivity [17, 18]. Previous work [10, 11] claims that nanocrystalline clusters existing in the amorphous matrix play an important role in the hard magnetic properties of these alloys. However, up to now, as the nanocrystalline clusters are not directly distinguishable in the x-ray diffraction (XRD) patterns and hard to investigate, the microstructure and magnetic thermostability of the alloy have not been intensively studied. In this work, we studied the microstructure and phase evolution upon annealing of an as-cast $Nd_{60}Al_{10}Fe_{20}Co_{10}$ cylindrical sample. The stability of the nanocrystalline clusters and the phase evolution, as well as related changes in magnetic properties of the samples, are presented. The relations between the stability of the nanocrystalline clusters and the coercivity, precipitation of Nd-rich metastable phase, and saturation magnetization are discussed.

Ingots with a nominal composition of $Nd_{60}Al_{10}Fe_{20}Co_{10}$ were prepared by arc melting of the elements Nd, Fe, Al, and Co with a purity of 99.9 at.% in a titanium-gettered Ar atmosphere. Cylinders 5 mm in diameter were prepared by suction casting under an argon atmosphere. The samples were taken from the central region of the cylinders and annealed in a furnace with a vacuum of 2.0×10^{-3} Pa. The structure of the samples was characterized by means of XRD in a Philips diffractometer using Cu Kα radiation. Scanning electron microscopy (SEM) was performed on a HITACHI S-570 SEM. A vibrating sample magnetometer (VSM) was used for the magnetic measurements of the as-cast and annealed samples. DSC measurements were carried out under a purified argon flow in a Perkin-Elmer DSC-7 at a heating rate of 10 K min^{-1}. The thermomagnetic (M–T) curves were obtained using a TA Instruments 2050 thermogravimetric analyser (TGA) under the influence of a permanent magnet. The sample was protected by purified nitrogen. The microstructural observation of the samples was carried out using a JEOL JEM-2010 high-resolution transmission electron microscope (HRTEM) with a Oxford LINK ISIS energy dispersive spectrometer (EDS).

Figure 1 shows the DSC trace (figure 1(a)) and the magnetic thermogravimetry curve (figure 1(b)) under the influence of a permanent magnet for the as-cast $Nd_{60}Al_{10}Fe_{20}Co_{10}$ BMG. Similarly to the findings for other BMGs, the typical sharp exothermic crystallization peak and endothermic melting peak are found in the DSC curve. In addition, there is a wide exothermic reaction peak ranging from 600 to 750 K, corresponding to a process of nucleation and growth, in the curve [12]. The magnetic thermogravimetry of the sample (i.e. magnetization of the sample) starts to increase gradually at about 650 K (much higher than the Curie temperature, as marked on the curve). This indicates that some magnetic phases precipitate from the amorphous matrix during the wide-peak exothermic reaction process.

Figure 2 presents the XRD patterns of the as-cast sample and samples annealed at 523, 623, 673, 723, and 793 K for 30 min. The scattering peaks in the XRD pattern of the as-cast sample (figure 2(a)) characterize the fully amorphous phase of the alloy within the XRD detection limit. Upon annealing at 523 K for 30 min, the XRD curve (figure 2(b)) does not show obvious change. Only some irregularities suggest that there might be some relaxed Nd-rich phases. The sample annealed at 623 K (figure 2(c)) exhibits clearly a few small peaks, which increase in intensity with annealing temperature from 623 to 723 K and disappear upon annealing at 793 K. This indicates the metastable precipitation of some crystalline phases. Meanwhile, there are some other stable crystalline phases coexisting with the metastable phases from 623 to 723 K (figure 2(c)–(e)), indicating that primary crystallization occurs within this temperature range. We could not identify the metastable and primary crystalline phases. Some of the reflections of these phases are in accordance with an unknown tetragonal phase reported previously [13–15]. The BMG fully crystallized upon annealing at 793 K, as shown in figure 2(f).

The SEM images of the above samples shown in figure 3 are roughly in accordance with the XRD results. The as-cast sample shows a single amorphous phase and the nanocrystalline

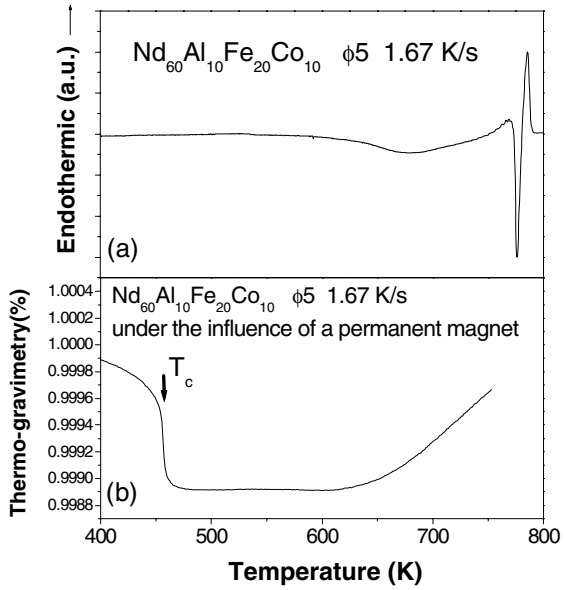

Figure 1. (a) The DSC trace and (b) magnetic thermogravimetry curve for as-cast $Nd_{60}Al_{10}Fe_{20}Co_{10}$ BMG.

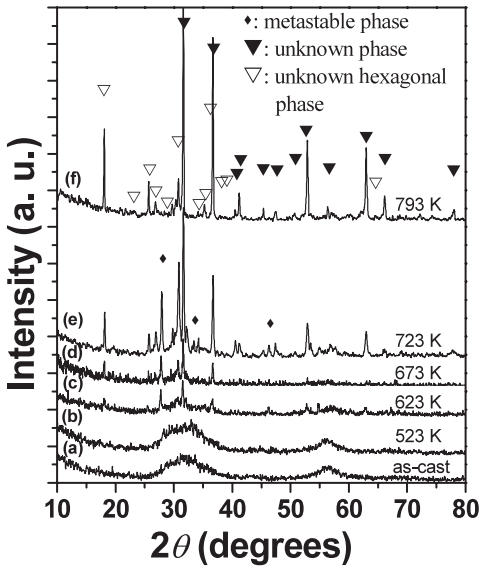

Figure 2. XRD patterns of the $Nd_{60}Al_{10}Fe_{20}Co_{10}$ BMG samples: (a) as-cast, (b) annealed at 523 K for 30 min, (c) annealed at 623 K for 30 min, (d) annealed at 673 K for 30 min, (e) annealed at 723 K for 30 min, and (f) annealed at 793 K for 30 min.

clusters are invisible within the SEM detection limit. No obvious precipitated phase can be found in the samples annealed at 523 and 623 K for 30 min. A lot of secondary-phase particles, as shown in figure 3(a), are found to distribute randomly in the matrix of the samples annealed at 723 K. These particles are the primary stable crystalline phase. The metastable phase

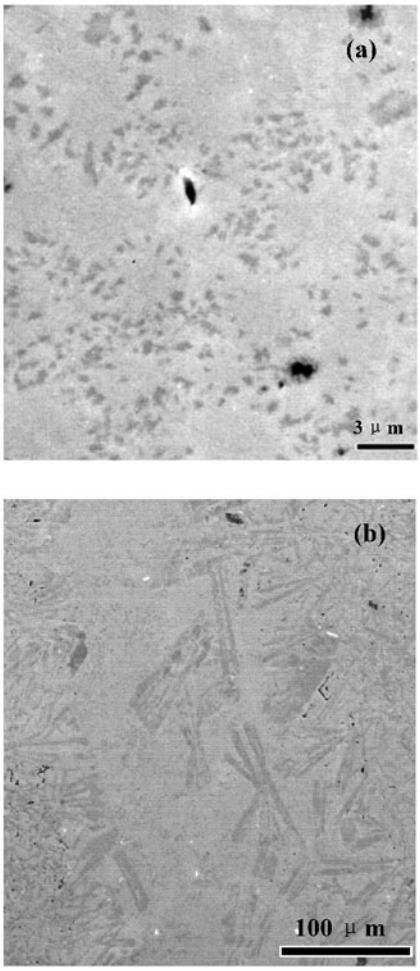

Figure 3. SEM images of the $Nd_{60}Al_{10}Fe_{20}Co_{10}$ samples annealed at (a) 723 K and (b) 793 K for 30 min.

reflected in the XRD patterns of the samples annealed at 623, 673, and 723 K is supposed to be present in too small an amount to be detected by SEM. The feature of equilibrium phases is shown in figure 3(b). The dendrites are detected as being Fe-rich phases with compositions of around $Fe_{52}Nd_{33}Al_{14}Co_3$, while the remainder has a composition of about $Nd_{65}Al_8Fe_{14}Co_{13}$.

Figure 4 illustrates the local structure of the sample annealed at 673 K for 30 min observed by HRTEM. Two kinds of crystalline phase can be observed. In most areas, nanocrystalline clusters with size 3–10 nm are found embedded in the amorphous matrix, as shown in figure 4(a). The crystal characters of these clusters are in accordance with those of the nanocrystalline clusters found in the as-cast rod. Furthermore, EDS results show that these clusters have a composition of about $Nd_{69}(Fe, Co)_{31}$, which is the same as the composition of the clusters in the as-cast rod [17] indicating that higher thermal stability of the nanocrystalline clusters in alloys. Meanwhile, some crystals different from above clusters are also found, as shown in figure 4(b). EDS results indicate that the crystal has a composition of about $Nd_{91}(Fe, Co)_9$. This does not match the composition of either the Fe-rich or the Nd-rich

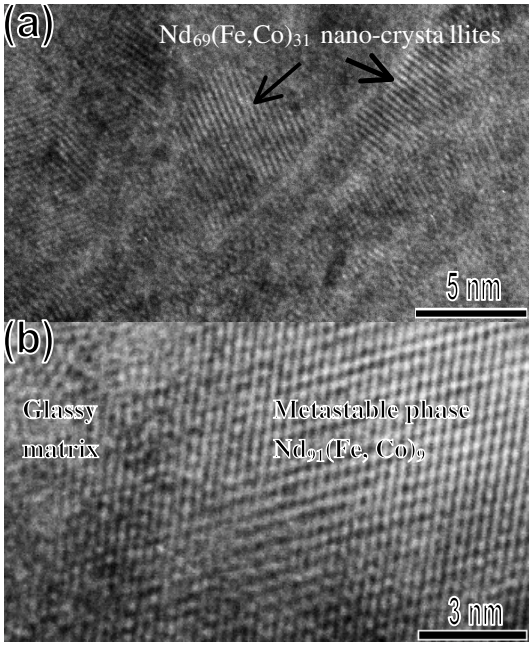

Figure 4. HRTEM images of (a) nanocrystalline clusters embedded in the amorphous matrix and (b) the metastable phase in a $Nd_{60}Al_{10}Fe_{20}Co_{10}$ rod sample annealed at 673 K for 30 min.

equilibrium phase in crystalline samples. These crystals could be the metastable phases appearing only in the temperature range from 623 to 723 K, according to the XRD patterns.

Figure 5(a) gives the hysteresis loops of the as-cast rod and samples annealed at different temperatures. The coercivities of the as-cast sample and the annealed samples are almost the same. But the magnetizations of these samples, as shown in figure 5(b), increase gradually from about 623 K. It is noted that there is a similarity between this magnetization–temperature dependence curve and the magnetic thermogravimetry curve above 600 K (shown in figure 1(b) and figure 5(b)). We infer that the increase of magnetization corresponds to the formation of the Nd-rich metastable phases, because some magnetic phases precipitate from the matrix when heated above 623 K and the crystalline sample containing equilibrium phases shows paramagnetic properties [18]. Earlier research on Zr–Ti–Cu–Ni–Be glass-forming alloy have found that the alloy would decompose into two amorphous phases near the calorimetric glass transition temperature to lower the free energy of the system [13]. The precipitation of the metastable phase and the primary crystallization in this BMG may also lower the free energy.

We attribute the coercivity of the samples to the presence of pre-existing nanocrystalline clusters in the BMGs. Previous work has observed that the coercivity is sensitive to the size and amount of these clusters [10, 16]. Schneider *et al* [10] have observed *in situ* formed finely dispersed nanocrystalline clusters of eutectic or near-eutectic composition in $Nd_{60}Fe_{30}Al_{10}$ glass-forming alloy and supposed that the structure observed might be related to phase separation in the undercooled liquid. Our recent results [17] on the Nd–Al–Fe–Co alloy system indicate that the formation of nanocrystalline clusters is closely related to the early-stage crystallization (at about 473 K) found in DSC traces of $Nd_{60}Al_{10}Fe_{20}Co_{10}$ melt-spun ribbons obtained at higher cooling rates. This kind of early-stage crystallization can also be found in the DSC curves of $Nd_{57}Al_{10}Fe_{20}Co_5B_8$ ribbons [19] and $Nd_{60}Fe_{30}Al_{10}$ ribbons

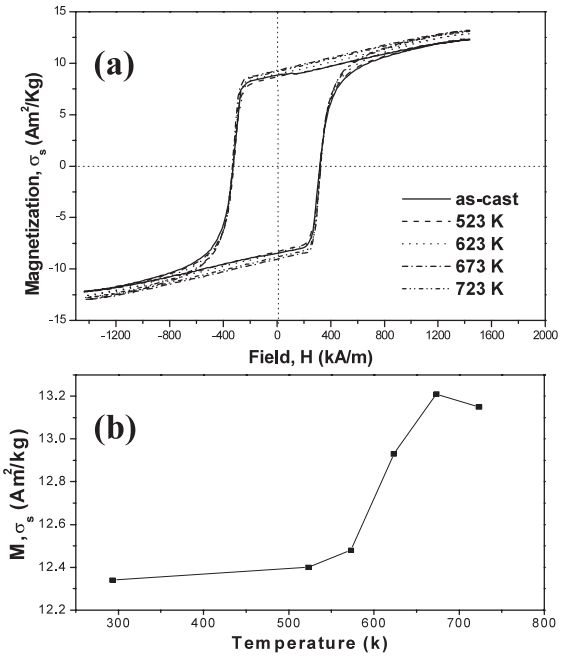

Figure 5. (a) Hysteresis loops of the $Nd_{60}Al_{10}Fe_{20}Co_{10}$ as-cast rod and rods annealed at 523, 623, 673, and 723 K for 30 min. (b) The dependence of the saturation magnetization on the annealing temperature.

(30 s^{-1}) [20] with much lower coercivity than their bulk counterparts. The absence of early-stage crystallization in the DSC curves of as-cast $Nd_{60}Al_{10}Fe_{20}Co_{10}$ bulk samples might be due to partial crystallization at the lower cooling rate. These partially crystallized phases are the nanocrystalline clusters in this work. Menushenkov *et al* [21] have reported that the Nd–Fe binary alloys with similar compositions of clusters are hard magnetic and have coercivities ranging from 320 to 360 kA m^{-1}, which is roughly equal to the value of the coercivity in the present work. Thus, the coercivity of the annealed samples depends on the existence and stability of nanocrystalline clusters. Compared with $Nd_{60}Fe_{30}Al_{10}$ bulk hard magnetic glass, $Nd_{60}Al_{10}Fe_{20}Co_{10}$ BMG exhibits higher coercivity and lower magnetization. The addition of Co to Nd–Fe–Al alloy is supposed to be useful for the improvement of the GFA by causing a strong reduction of the melting temperature [14]. In our opinion, Co addition might also enhance the glass transition temperature of the alloys and simultaneously increase the content of partially crystallized phases (nanocrystalline clusters) with higher coercivity and lower magnetization than the amorphous matrix.

In summary, the nanocrystalline clusters which induce the hard magnetism of as-cast $Nd_{60}Al_{10}Fe_{20}Co_{10}$ BMG have high thermal stability upon annealing prior to main crystallization process. The high stability of the nanocrystalline clusters is deduced to be due to their eutectic or near-eutectic composition of about $Nd_{69}(Fe, Co)_{31}$. During the annealing process, primary crystallization occurs in the $Nd_{60}Al_{10}Fe_{20}Co_{10}$ BMG with the precipitation of metastable phase and primary crystalline phases. The precipitation of Nd-rich metastable phase (with a composition of about $Nd_{91}(Fe, Co)_9$) enhances the saturation magnetization. The equilibrium phases in the crystalline sample have compositions of about $Fe_{52}Nd_{33}Al_{14}Co_3$ and $Nd_{65}Al_8Fe_{14}Co_{13}$.

Acknowledgment

The authors are grateful for the financial support from the National Natural Science Foundation of China (Grant Nos 50031010, 59925101 and 59971028).

References

[1] Volkert C A and Spaepen F 1989 *Acta Metall.* **37** 1355
[2] Zhu J, Clavaguera-Mora M T and Clavaguera N 1997 *Appl. Phys. Lett.* **70** 1709
[3] Van den Beukel A and Sietsma J 1994 *Mater. Sci. Eng.* A **179/180** 86
[4] Zhuang Y X and Wang W H 2000 *J. Appl. Phys.* **87** 8209
[5] Johnson W L 1999 *MRS Bull.* **24** 42
[6] Greer A L 1995 *Science* **267** 1947
[7] Inoue A 2000 *Acta Mater.* **48** 279
[8] Wang W H, Wei Q and Bai H Y 1997 *Appl. Phys. Lett.* **71** 58
[9] Hays C C, Kim C P and Johnson W L 2000 *Phys. Rev. Lett.* **84** 2901
[10] Schneider S, Bracchi A, Samwer K, Seibt M and Thiyagarajan P 2002 *Appl. Phys. Lett.* **80** 1749
[11] Delamare J, Lemarchand D and Vigier P 1994 *J. Alloys Compounds* **216** 273
[12] Fecht H J 1995 *Mater. Trans. JIM* **36** 777
[13] Fan G J, Löser W, Roth S, Eckert J and Schultz L 1999 *Appl. Phys. Lett.* **75** 2984
[14] Fan G J, Löser W, Roth S, Eckert J and Schultz L 2000 *Mater. Res.* **15** 1556
[15] Ding J, Si L, Li Y and Wang X Z 1999 *Appl. Phys. Lett.* **75** 1763
[16] Wei B C, Wang W H, Pan M X, Han B S and Zhang Z R 2001 *Phys. Rev.* B **64** 012406
[17] Xia L, Wei B C, Zhang Z, Pan M X, Zhao D Q, Wang W H and Dong Y D 2003 *J. Phys. D: Appl. Phys.* **36** 775
[18] Pan M X, Wei B C, Xia L, Wang W H, Zhao, D Q, Zhang Z and Han B S 2002 *Intermetallics* **10** 1215
[19] Xing L Q, Eckert J, Löser W, Roth S and Schultz L 2000 *J. Appl. Phys.* **88** 3565
[20] Wang X Z, Li Y, Ding J, Si L and Kong H Z 1999 *J. Alloys Compounds* **290** 209
[21] Menushenkov V P, Andersen S J and Høier R 1998 *Proc. 10th Int. Symp. on Magnetic Anisotropy and Coercivity in Rare-Earth Transition Metal Alloys (Dresden, 1998)* p 97